# A Framework for Dyadic Physical Interaction Studies during Ankle Motor Tasks

Sangjoon J. Kim†, Yue Wen†, Emek Barış Küçüktabak, Shaobo Zhan, Kevin Lynch, Levi Hargrove, Eric J. Perreault, and Jose L. Pons

***Abstract*—Over the past few decades, there have been many studies of human-human physical interaction to better understand why humans physically interact so effectively and how dyads outperform individuals in certain motor tasks. Because of the different methodologies and experimental setups in these studies, however, it is difficult to draw general conclusions as to the reasons for this improved performance. In this study, we propose an open-source experimental system for the systematic study of the effect of human-human interaction, as mediated by robots, at the ankle joint. We also propose a new framework to study various interactive behaviors (i.e., collaborative, cooperative, and competitive tasks) that can be emulated using a virtual spring connecting human pairs. To validate the proposed experimental framework, we perform a transparency analysis, which is closely related to haptic rendering performance. We compare muscle EMG and ankle motion data while subjects are barefoot, attached to the unpowered robot, and attached to the powered robot implementing transparency control. We also validate the performance in rendering virtual springs covering a range of stiffness values (5-50 Nm/rad) while the subjects track several desired trajectories (sine waves at frequencies between 0.1 and 1.1 Hz). Finally, we demonstrate the feasibility of the system in studying human-human interaction under different interactive behaviors.**

***Index Terms*—Physical human-robot interaction, haptics and haptic interfaces, human-robot teaming, human factors and human-in-the-loop.**

Manuscript received: February, 24, 2021; Revised May, 19, 2021; Accepted June, 17, 2021.

This paper was recommended for publication by Editor Gentiane Venture upon evaluation of the Associate Editor and Reviewers' comments.

This work was supported by National Science Foundation / National Robotics Initiative (Grant No: 2024488).

† These two authors contributed equally to the work.

S. J. Kim and Y. Wen are with the Legs and Walking Lab of Shirley Ryan AbilityLab and the Department of Physical Medicine and Rehabilitation, Feinberg School of Medicine, Northwestern University, Chicago, IL, USA.

E. B. Küçüktabak and S. Zhan are with the Legs and Walking Lab of Shirley Ryan AbilityLab and the Department of Mechanical Engineering, McCormick School of Engineering, Northwestern University, Evanston, IL, USA.

K. Lynch is with the Center for Robotics and Biosystems and the Department of Mechanical Engineering, McCormick School of Engineering, Northwestern University, Evanston, IL, USA.

L. Hargrove is with the Center for Bionic Medicine (CBM) of Shirley Ryan AbilityLab and Department of Physical Medicine and Rehabilitation, Feinberg School of Medicine, Northwestern University, Chicago, IL,USA.

E. J. Perreault is with the Department of Physical Medicine and Rehabilitation, Feinberg School of Medicine, Northwestern University, Chicago, IL, USA.

J. L. Pons (corresponding author) is with the Legs and Walking Lab of Shirley Ryan AbilityLab, Department of Mechanical Engineering and Department of Biomedical Engineering, McCormick School of Engineering, and Department of Physical Medicine and Rehabilitation, Feinberg School of Medicine, Northwestern University, Chicago, IL, USA, e-mail: jpons@sralab.org

Digital Object Identifier (DOI): see top of this page.

## I. Introduction

HUMANS often physically interact with one another to accomplish tasks that are difficult to do alone (e.g., moving a mattress) or to exchange information for learning new tasks (e.g., athletic training, rehabilitation). Interestingly, it has been shown in many studies that the physical interaction between human pairs leads to improvements in the shared task performance and/or in individual motor learning when compared to performing the same task alone [1]–[15]. The underlying mechanisms governing motor performance improvement in human-human physical interaction have drawn the interest of many researchers during the past few decades.

Early studies were conducted using simple passive mechanical devices such as a two-handled crank where physical information was directly exchanged between pairs [8], [9] or using sensors to quantify a pair's ability to replicate forces they have perceived with their index fingers [10]. Recently, more complex dyadic behaviors have been explored using robotic devices to control the interaction dynamics between two or more humans [1]–[7], [11], [12]. Virtual connections between humans are typically modeled as springs or dampers.

With the help of robotic devices, several studies have been conducted to investigate the effect of physical interaction on shared motor tasks [1]–[3], [6], [11]. Ganesh et al [1] showed that when human pairs collaborate to track an identical moving target on a monitor with separate manipulators that are virtually connected, the interaction is mutually beneficial, specifically, both interacting partners improve shared task performance and individual motor learning. Similarly, in the study of Takagi et al. [2], robotic devices were used to investigate collaborative physical interaction when two participants track a target using wrist flexion/extension for varying virtual stiffnesses. It has been shown that tracking performance increased for the less skilled partner, who had higher tracking error, at the cost of the skilled partner's muscular effort. A follow-up study by Takagi et al. [11] showed that when multiple (i.e., triad, tetrad) individuals were connected during a 2D horizontal planar tracking task where individuals were asked to track targets on a computer screen with haptic devices, the interaction benefits increased with the group size when additional individuals were virtually connected.

Different results have been presented related to the effects of physical interaction on task performance and motor learning [3], [6]. Che et al. [3] reported that for a tracking task in which the pairs were asked to track a target with linear movement, while holding manipulators, the stiffness of the virtual

connection influences the task performance and individual motor learning. While stiffer connections led to improvements, weaker connections did not lead to significant improvement in terms of task performance or motor learning. Another study by Beckers et al. [6] showed that for the tracking of stationary targets with cursors controlled by hand-held manipulators, task performance with physical collaboration was significantly better, however, physical interaction did not improve individual motor learning.

Discrepancies in experimental tasks and setups make it difficult to generalize across published results, yielding few clear conclusions as to how motor improvement are obtained through physical interactions. There are also limited studies that compare how different interactive behaviors (i.e., collaborative, cooperative, or competitive tasks) and the characteristics of the virtual connection may affect task performance and motor learning. Therefore, it is important to systematically investigate the effect of each interaction variable.

To this end, we propose an open-source framework that will be shared with the community to study different forms of dyadic interaction (i.e., different interaction behaviors and level of virtual connections). This will allow others to reproduce the results presented in this study and to build upon the proposed framework. We also designed our study based on lower extremity motor tasks to investigate if and how motor improvements, presented in previous upper extremity studies, can be generalized and translated to the lower extremity. We first introduce the implementation of an interaction torque controller. We then introduce the implementation of a haptic rendering environment that is used to provide virtual connections between two ankle robots. With the haptic rendering environment, we emulate three types of interactive tasks — collaborative, cooperation, and competition tasks — using different interaction spring parameters. Finally, we showcase the framework with three different interactive conditions and analyze how different interactive behaviors a may effect task performance.

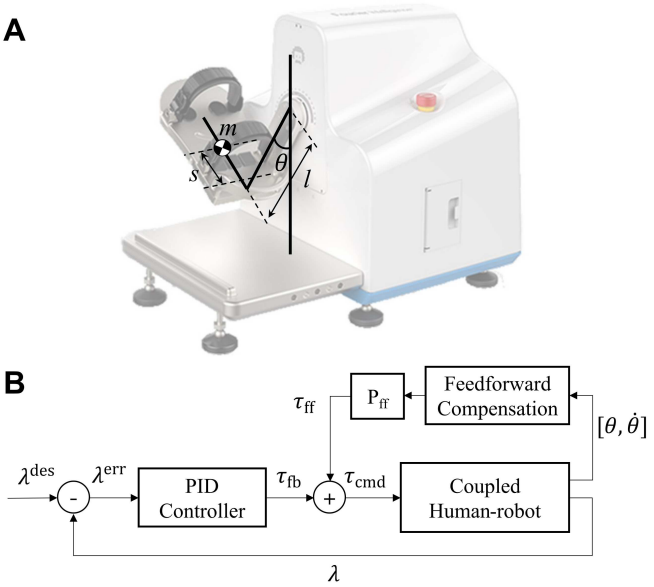


Fig. 1. (A) M1 device. Variables used for the feedforward model are presented. (B) The interaction torque control loop. $\lambda^{\text{des}}$: desired interaction torque, $\lambda^{\text{err}}$: interaction torque error, $\tau_{\text{fb}}$: feedback torque, $\tau_{\text{ff}}$: feedforward torque, $\tau_{\text{cmd}}$: command torque

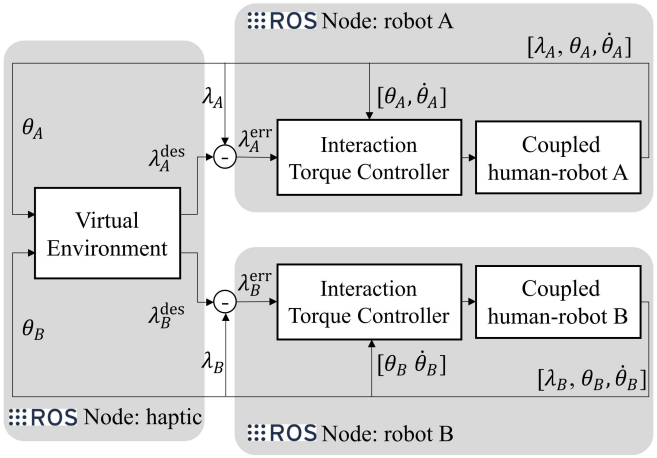


Fig. 2. Scheme of multi-M1 interaction.

## II. Infrastructure Development

### A. Description of the M1 ankle rehabilitation robot

We used commercially-available ankle robots (M1, Fourier Intelligence, China) that were developed to provide ankle joint rehabilitation for patients with stroke or spinal cord injury (SCI) as shown in Fig. 1A. The M1 device consists of an AC servo motor (SMC60S, Kinco Motor, China) with a 69:1 gear box (MF60XL2, VGM, Taiwan) that can apply motor torque to the ankle joint; a torque sensor (JNNT-F, JN, China) that can be used to measure the interaction torque between the user's ankle joint and the M1 device; and a magneto-electric encoder that can be used to measure the angular position of the ankle joint. An open-source robotic development software stack called CORC [16] was developed and used for real-time control and feedback signal visualization.

### B. Implementation of an interaction torque controller

An interaction torque controller was developed to render high-resolution virtual physical environments during dyadic interaction and to allow transparent motion for individual use. This controller has a feedforward term to compensate for modeled frictional and gravitational terms, and a feedback term that depends on the interaction torque error to compensate for model discrepancies and unmodeled dynamics. The interaction torque control loop is shown in Fig. 1B. The torque command ($\tau_{\text{cmd}}$), used to control the AC servo motor of the M1 device, is calculated by the sum of the feedforward ($\tau_{\text{ff}}$) and feedback ($\tau_{\text{fb}}$) terms as follows,

$$\tau_{\text{cmd}} = \tau_{\text{ff}} + \tau_{\text{fb}} \tag{1}$$

The feedforward term ($\tau_{\text{ff}}$) was estimated by modeling the dynamic and static friction of the system using the following equation,

$$\tau_{\text{ff}} = P_{\text{ff}}[msg\sin(\theta) + mlg\cos(\theta) + c_0\dot{\theta} + c_1\,\text{sgn}(\dot{\theta})] \tag{2}$$

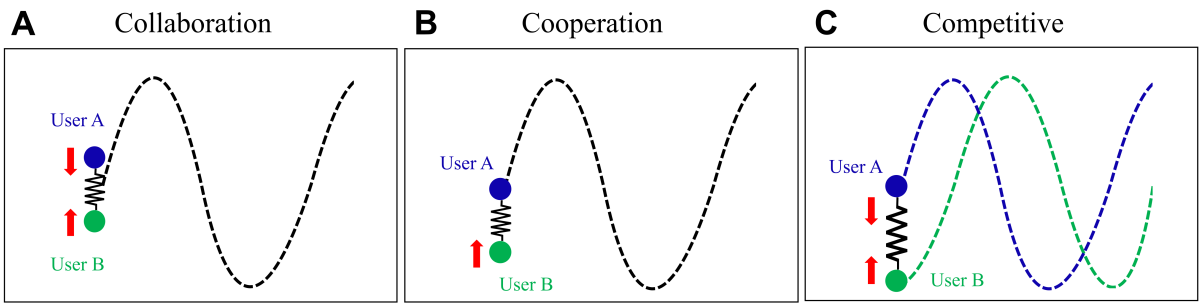


Fig. 3. Framework of three interactive behaviors. Note that the rest length of all of the springs is zero. (A) During collaborative behaviors, the dyads attempt to track identical desired trajectories and there is an attractive spring that connects the pair. (B) During cooperative (teacher-student) behaviors, the dyads attempt to track identical desired trajectories and there is a unidirectional attractive spring so that only one participant can affect the other. (C) During competitive mode, each participant attempts to track a different trajectory. There is an attractive spring between the two participants so that each participant impedes the other participant. The red arrows represent force induced by the virtual springs.

where $\theta$ is the angular position, $\dot{\theta}$ is the angular velocity, $c_0$ is the dynamic friction coefficient, $c_1$ is the static friction, $m$ is the mass of the footplate, $s$ and $l$ are the moment arms, $g$ is the gravitational acceleration, and $P_{\text{ff}}$ is a constant gain. Note that $\theta$ is defined with respect to the axis defined in Fig. 1A. To estimate $c_0$, $c_1$, $s$, and $m$, we measured the M1's trajectory in response to given torque profiles and used MATLAB's `lsqcurvefit` function to fit the parameters. We introduce a constant gain, $P_{\text{ff}}$, to allow a percentage of the plant dynamics to be compensated as part of controller tuning.

The feedback term ($\tau_{\text{fb}}$) was calculated using the following equation,

$$\tau_{\text{fb}} = P_{\text{fb}}\lambda^{\text{err}} + I_{\text{fb}}\int \lambda^{\text{err}} dt + D_{\text{fb}}\dot{\lambda}^{\text{err}} \tag{3}$$

where $\lambda^{\text{err}}$ is the interaction torque between the user's ankle joint and the M1 device, and $P_{\text{fb}}$, $I_{\text{fb}}$, and $D_{\text{fb}}$ are constant gains.

After identifying the coefficients of $\tau_{\text{ff}}$, we first heuristically tuned the proportional gain of the feedforward term $P_{\text{ff}}$, then the proportional $P_{\text{fb}}$, derivative gain $D_{\text{fb}}$, and integral gain $I_{\text{fb}}$ of the PID controller to minimize resistive torque and oscillation felt by the user. The feedforward model parameters and feedback PID gains are summarized in Table I.

TABLE I
PARAMETERS OF THE FEEDFORWARD AND FEEDBACK MODEL.

| Category | Symbol | Value [Unit] |
|---|---|---|
| Static friction | $c_0$ | 0.27 [Nm] |
| Dynamic friction coefficient | $c_1$ | 0.28 [Nm/rad] |
| Foot plate mass | $m$ | 1.08 [kg] |
| Constant feedforward term gain | $P_{\text{ff}}$ | 0.7 |
| Proportional gain of the feedback loop | $P_{\text{fb}}$ | 0.26 [Nm/rad] |
| Integral gain of the feedback loop | $I_{\text{fb}}$ | 0.05 [Nm/rad/s] |
| Differential gain of the feedback loop | $D_{\text{fb}}$ | 0.02 [Nm*s/rad] |

### C. Implementation of a haptic virtual environment

Two M1 devices were connected to the same PC where all the computations for interaction torque control and virtual environment rendering were done. M1 robots were run as local ROS nodes under the application layer of CORC, and another local node was created for the virtual physical environment rendering. This additional node subscribes to the states of the robots, calculates the desired interaction torque for each robot according to the virtual environment dynamics, and publishes those values. Robot nodes subscribe to their corresponding desired interaction torque messages and use them as the references for their interaction torque controllers. This scheme is presented in Fig. 2.

To obtain virtual connections between two M1 devices, we calculated the desired interaction torque $\lambda^{\text{des}}$ that depends on spring stiffness ($K_{\text{virt}}$) and angular position of each user ($\theta_{\text{A}}$, $\theta_{\text{B}}$). The taxonomy proposed by Jarrasse et al., was adopted to design the framework of interactive behaviors: collaboration, competition, and cooperation [17]. Each interactive behavior is defined and implemented as follows (see Fig. 3):

- **Collaboration**: *Both users jointly try to solve a common problem.* This is implemented with an attractive virtual spring between the ankle angular position of the two users. User A is pulled towards the angular position of User B and User B is pulled towards User A:

$$\lambda_i^{\text{des}} = K_{\text{virt}}(\theta_j - \theta_i) \quad i,j \in \{\text{A},\text{B}\},\, i \neq j \tag{4}$$

  Both users have identical desired trajectories.
- **Cooperation (teacher-student)**: *Different roles are assigned to the users prior to the beginning of a task. The teacher can correct the student.* This is implemented with a unidirectional virtual spring between the ankle angular position of the two users. User B is pulled towards the angular position of User A, but User B cannot affect User A:

$$\lambda_{\text{A}}^{\text{des}} = 0, \quad \lambda_{\text{B}}^{\text{des}} = K_{\text{virt}}(\theta_{\text{A}} - \theta_{\text{B}}) \tag{5}$$

  Both users have identical desired trajectories.
- **Competition**: *Both users focus on their own action and effort, and if necessary impede the other's performance.* This is implemented by providing conflicting desired trajectories to each user as shown in Fig. 3C. Similar to collaboration, a virtual spring between the ankle angular position of the two users is implemented.

The development code to implement the interaction torque controller and haptic virtual environment can be accessed at https://github.com/ywen3/CANOpenRobotController.

### D. Validation of system transparency

The transparency (i.e., dynamic back-drivability) of the M1 device with the interactive torque controller was validated. The electromyography (EMG) signals of the ankle flexor and extensor muscles and the angular position of the ankle joint of three healthy participants (mean ± standard deviation; age 27.3 ± 3.5 years, height 176.3 ± 4.9 cm, body mass 73.3 ± 10.6 kg, 3 males) were analyzed during cyclical ankle movements at 1 Hz through the full ankle range of motion (ROM). Participants performed the cyclical movement based on audio cue provided by a metronome. Three conditions were compared: (1) barefoot ($BF$) with no robot, as a baseline; (2) wearing the M1 with no power ($M1_{\text{OFF}}$); and (3) wearing the M1 with transparency control ($M1_{\text{ON}}$). For $M1_{\text{ON}}$, the desired interaction torque ($\lambda^{\text{des}}$) was set equal to zero. Two bipolar EMG electrodes (MA400 EMG Systems, Motion Lab Systems, USA) were placed on the belly of the medial gastrocnemius (GAS) and tibialis anterior (TA) muscles after cleaning the skin with alcohol. The angular position of the ankle joint was measured using a motion capture camera system (6 Hawk motion capture cameras, Motion Analysis, USA). The EMG signals were sampled at 1500 Hz and the motion data was sampled at 100 Hz. Raw EMG signals were bandpass filtered to reduce the influence of motion artifacts and high-frequency background noise (6th-order Butterworth filter with a cutoff frequency of 10 and 500 Hz) and a notch filter to remove power-line interference (2nd-order IIR filter at 60 Hz with a bandwidth of 1 Hz) [18]. We calculated the mean absolute value (MAV) of the rectified and low-pass-filtered signals (6th-order Butterworth filter with a cutoff frequency of 10 Hz) to compare the three conditions. The high-frequency noise of the motion data was filtered using a 6th-order Butterworth filter with a cutoff frequency of 6 Hz [19].

### E. Validation of the haptic rendering environment

To validate the performance of rendering virtual connections, we conducted two experiments: (1) performance of rendering a virtual spring on a single robot and (2) feasibility of systematically investigating different interactive conditions.

*1) Performance of rendering a virtual spring:* To render a virtual spring, the desired torque ($\lambda^{\text{des}}$) is defined as

$$\lambda^{\text{des}} = K_{\text{virt}}(\theta - \theta_{\text{e}}) \tag{6}$$

where $\lambda^{\text{des}}$ is the desired torque and $K_{\text{virt}}$ and $\theta_e$ are the stiffness and equilibrium position of the virtual spring, respectively.

To validate the haptic rendering performance, we tested the rendering accuracy for different virtual stiffness levels and different frequencies of the motion trajectory to be tracked. We set the equilibrium position of the virtual spring, and asked a participant to don the M1 device and stretch the virtual spring away from the equilibrium position with his ankle. Specifically, we set the equilibrium position, $\theta_{\text{e}}$, to 0.55 rad (see Fig. 1A), which is approximately the center position of the ankle range of motion. We then verified the virtual spring rendering performance with ten virtual stiffness levels ($K_{\text{virt}}$), 5 to 50 Nm/rad with 5 Nm/rad increments. For each condition,

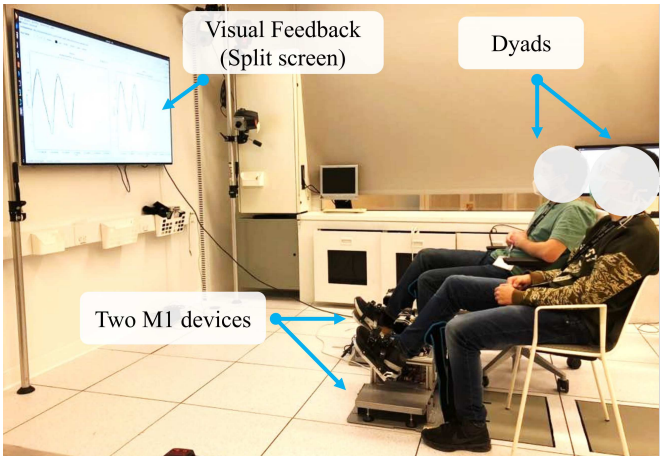


Fig. 4. Experimental setup for the feasibility test of dyadic studies.

we asked the participant to track a sine wave trajectory with his ankle angular position given through visual feedback. The amplitude of the sine wave was 0.4 rad to cover the range of motion of the ankle during natural gait [20]. The frequency of the sine wave was fixed at 0.3 Hz. We also tested the haptic rendering performance for different desired trajectory frequencies. We fixed the virtual stiffness level to 25 Nm/rad and changed the sine wave frequency from 0.1 to 1.1 Hz with 0.2 Hz increments. During the experiment, we recorded the joint angle ($\theta$), desired interaction torque ($\lambda^{\text{des}}$), and actual interaction torque ($\lambda$) for 10 tracking cycles.

We analyzed the rendering performance of a virtual spring by calculating the normalized root-mean-square error (NRMSE) between the desired interaction torque induced by the virtual spring and the actual interaction torque induced to the ankle by the virtual stiffness,

$$\begin{aligned} RMSE_{\lambda} &= \sqrt{\frac{\sum_{n=1}^{N}(\lambda^{\text{des}}(n) - \lambda(n))^2}{N}} \\ NRMSE_{\lambda} &= \frac{RMSE_{\lambda}}{\lambda^{\text{des}}_{\text{max}} - \lambda^{\text{des}}_{\text{min}}} \end{aligned} \tag{7}$$

where $\lambda^{\text{des}}$ is the desired interaction torque, $\lambda$ is the measured interaction torque, and $N$ is the number of samples in each testing trials. The $\lambda^{\text{des}}_{\text{max}}$ and $\lambda^{\text{des}}_{\text{min}}$ are the maximum and minimum value of desired interaction torque, respectively.

*2) Feasibility of systematically investigating different interactive conditions:* To demonstrate the feasibility of the proposed infrastructure in investigating the effect of different interactive behaviors, we test collaborative, cooperative, and competitive behaviors for a given virtual stiffness level ($K_{\text{virt}}$ = 20 Nm/rad). Two healthy participants (mean ± standard deviation: age 27.5 ± 4.9 years, height 173.0 ± 1.4 cm, body mass 70.0 ± 8.5 kg, 2 males) were seated next to each other and were each asked to don an M1 device. Both participants familiarized themselves with the device while the devices operated in transparency mode ($\lambda^{\text{des}} = 0$). Then the participants were asked to perform a tracking task with their ankle based on visual feedback provided via a monitor. The visual feedback was provided in the form of a split screen

This article has been accepted for publication in a future issue of this journal, but has not been fully edited. Content may change prior to final publication. Citation information: DOI 10.1109/LRA.2021.3092265, IEEE Robotics and Automation Letters



where each user was provided with only the desired trajectory and his/her own ankle angular position. The experimental setup is shown in Fig. 4.

For the collaborative and cooperative conditions, both participants were asked to track an identical sine waveform. We changed the amplitude and frequency of the sine waveform every two cycles to increase the difficulty of the tracking task and to introduce learning effects. We selected the amplitude and frequency based on uniform random number generators with ranges of [0.3, 1.2] rad and [0.15, 0.45] Hz, respectively. For the competitive condition, one participant was asked to track a sine waveform, while the other participant tracked a cosine waveform of the same frequency and amplitude. A new amplitude and frequency were selected randomly for every two cycles of the sine/cosine waveform. The seed of the random number generator was changed for each interactive behavior. A total of five trials was tested for each interactive behavior, and during each trial participants were ask to track 10 cycles of the waveform. Between each interactive condition, the pair was provided five minutes of rest, and between each trial, one minute of rest. In the cooperative condition, in order to have a teacher-student relationship, the partner selected as the "teacher" practiced the trajectory for five trials before interacting with the "student," who had not practiced. For the collaborative condition, both participants were new to the tracking trajectories. During experiments, we recorded the target trajectory, actual trajectory, and interaction torque from both participants. The tracking performance was quantified by the root-mean-square error (RMSE) between the desired tracking trajectory and actual tracking trajectory,

$$RMSE_\theta = \sqrt{\frac{\sum_{n=1}^{N}(\theta^{\text{des}}(n) - \theta(n))^2}{N}} \tag{8}$$

where $\theta^{\text{des}}$ is the desired trajectory, $\theta$ is the actual tracking trajectory of the dyads (i.e., either $\theta_{\text{A}}$ or $\theta_{\text{B}}$), and $N$ is the number of data samples in each trial (i.e., 10 tracking cycles).

The institutional review board (IRB) of the Northwestern University approved this study (STU00212684) and all procedures were in accordance with the Declaration of Helsinki.

## III. Results

### A. System transparency

To validate system transparency, we compared the MAV of the EMG data measured from the TA and GAS muscles for three participants during ankle movement under (1) $BF$, (2) $M1_{\text{OFF}}$ and (3) $M1_{\text{ON}}$ conditions. We calculated the mean EMG of each condition over 10 repetitions for each participant and normalized the mean of $M1_{\text{OFF}}$ and $M1_{\text{ON}}$ conditions by the $BF$ condition as shown in Fig. 5A and B. For the $M1_{\text{OFF}}$ condition, approximately 3.90 $\pm$ 1.06 and 1.55 $\pm$ 0.43 times more muscle effort was required compared to the $BF$ condition for the TA and GAS muscle, respectively. For the $M1_{\text{ON}}$ condition, the normalized mean EMG of the TA and GAS muscles were 0.96 $\pm$ 0.04 and 0.79 $\pm$ 0.22, respectively, which indicates that similar or less muscle effort is required to move the ankle as compared to the $BF$ condition using the proposed interaction torque controller. Fig. 5C shows the range of motion of the ankle that was used in each condition for the three participants.

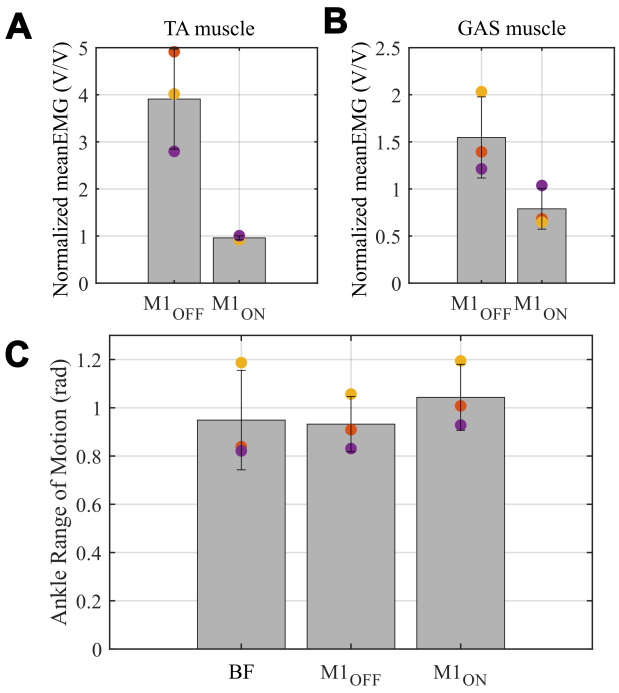


Fig. 5. System transparency result. The colored circles denote each participant. (A) Mean EMG data of the TA muscle for $M1_{\text{OFF}}$ and $M1_{\text{ON}}$ condition normalized by the $BF$ condition. (B) Mean EMG data of the GAS muscle for $M1_{\text{OFF}}$ and $M1_{\text{ON}}$ condition normalized by the $BF$ condition. (C) The range of motion of the ankle during each condition.

### B. Haptic rendering performance

*1) Performance of rendering a virtual spring:* The rendered interaction torque follows the desired interaction torque with the interaction torque controller using both feedback and feedforward compensation (Fig. 6A). The NRMSE$_\lambda$ between the rendered interaction torque and desired interaction torque was quantified across different stiffness levels and tracking tasks with varying frequencies. The NRMSE$_\lambda$ generally decreases as the virtual stiffness increases (Fig. 6C). The mean and standard deviation of NRMSE$_\lambda$ from all testing stiffness levels are 5.55 $\pm$ 1.83%. The rendered stiffness was slightly smaller than the desired stiffness (Fig. 6B). The ratio between the rendered stiffness and desired stiffness across all stiffness levels was 0.86 $\pm$ 0.04. With a fixed stiffness level (i.e., at 25 Nm/rad), the NRMSE$_\lambda$ increased as the frequency of the tracking task increased (Fig. 6D). The mean and standard deviation of the NRMSE$_\lambda$ from all testing frequencies were 7.03 $\pm$ 3.01%. Participants also reported that they felt that the M1 device was acting like a spring and they were able to recognize different stiffness values during the experiments.

*2) Feasibility of systematically investigating different interactive behavior:* The average position error between the two dyads for each interactive behavior was calculated across the five trials. Specifically, the averaged position error between the two dyads were 0.030$\pm$0.007 rad for the collaborative tasks, 0.037$\pm$0.007 rad for the cooperative tasks, and 0.306$\pm$0.012

This article has been accepted for publication in a future issue of this journal, but has not been fully edited. Content may change prior to final publication. Citation information: DOI 10.1109/LRA.2021.3092265, IEEE Robotics and Automation Letters



rad for the competitive tasks. The average interaction torque across the five trials and two participants were 0.57±0.05 Nm and 5.52±0.10 Nm for collaborative and competitive tasks, respectively. The average interaction torque across the five trials of the novice (student) in the cooperation tasks was 0.59±0.09 Nm. The higher position error between the two dyads during the competitive tasks introduced higher interactive torque compared to the other two interactive behaviors as participants had different tracking goals.

The difference between the fifth trial and the first trial of the averaged tracking $\text{RMSE}_\theta$ for each interactive behavior was also calculated. Specifically, the average change across the two participants in tracking $\text{RMSE}_\theta$ between the fifth trial and the first trial was 0.024 ± 0.004 rad for collaborative tasks, 0.038 ± 0.001 rad for cooperative tasks, and 0.015 ± 0.007 rad for competitive tasks (Fig. 7A-C).

## IV. Discussion

### A. Interaction torque controller

One drawback of the proposed interaction torque controller is the need to tune four parameters (i.e., $P$, $I$, $D$, $P_{\text{ff}}$). The performance of these parameters across different test subjects and different virtual spring stiffness may not be consistent. For example, as shown in Fig. 5B, depending on the tuned parameters, overcompensation may occur. For two participants, the transparency controller reduced the GAS muscle effort needed to move the ankle beyond what was required to move the bare foot. This may lead to motion instability or distortion in the natural motion. To avoid such issues, a higher-level feedback loop that depends on the rendered spring error or some auto-tuning methods [21]–[23] can be implemented in the future. Another possible improvement is to use an IMU on the footplate to compensate for the inertial forces due to acceleration [24] or to implement an admittance controller at the acceleration level [25].

### B. Haptic rendering environment

*1) Performance of rendering a virtual spring:* There are several sources of error for rendering the virtual spring. We observed that the rendered virtual stiffness is smaller than the desired virtual stiffness, which might be due to the manual tuning of the PID controller. We tuned the feedforward gain and feedback gains specifically for $K_{\text{virt}} = 25$ Nm/rad, which led to larger $\text{NRMSE}_\lambda$ for other virtual stiffnesses. Also, relatively higher errors were observed for lower virtual stiffnesses. When identical angle deviation was induced, the desired interaction torque was smaller with a lower virtual stiffness (e.g., 5 Nm/rad). This led to a larger sensor noise to desired torque ratio, which resulted in larger $\text{NRMSE}_\lambda$. The $\text{NRMSE}_\lambda$ also increased with higher tracking trajectory frequencies induced to the virtual spring. This was mainly because the actuation system was not able to respond to higher excitation frequencies, which also caused a higher $\text{NRMSE}_\lambda$.

*2) Feasibility of dyadic physical interaction studies:* In this study, we only performed the dyadic feasibility experiment for a single dyad to demonstrate the capability in testing different interactive behaviors with the proposed infrastructure.

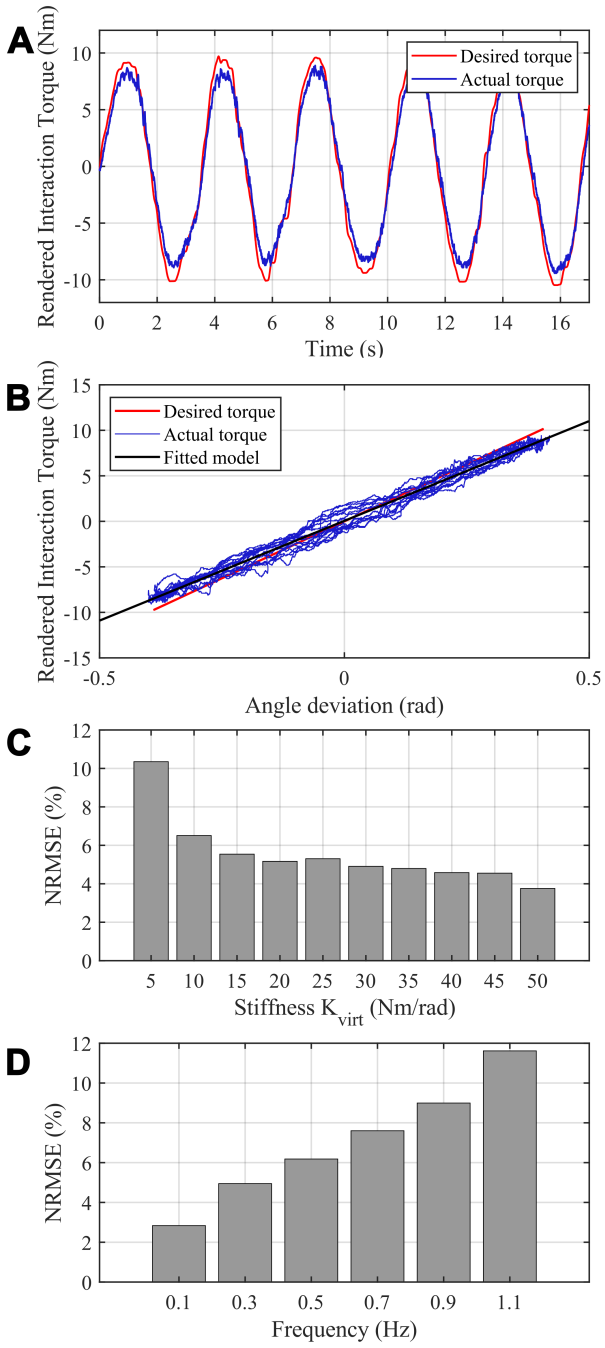


Fig. 6. Haptic rendering results. (A) The desired and actual rendered torque. (B) The desired and actual rendered torque are proportional to the angular deviation with a slope of the virtual stiffness. (C) Summary of the $\text{NRMSE}_\lambda$ between the desired and actual rendered torque for ten stiffness levels under tracking frequency of 0.3 Hz and amplitude of 0.4 rad. (D) The $\text{NRMSE}_\lambda$ between the desired and actual torque for different excitation frequencies. Note that the virtual stiffness used in (A), (B) and (D) is 25 Nm/rad.

Therefore, in order to generalize any results of motor learning presented in Fig. 7A-C, additional experimental work and further exploration are required.

There are several limitations of the current experimental protocol. For each interactive behavior, we changed the seed of the random number generator that was used to create a new desired tracking trajectory (see Fig. 7D-F). The seed

This article has been accepted for publication in a future issue of this journal, but has not been fully edited. Content may change prior to final publication. Citation information: DOI 10.1109/LRA.2021.3092265, IEEE Robotics and Automation Letters



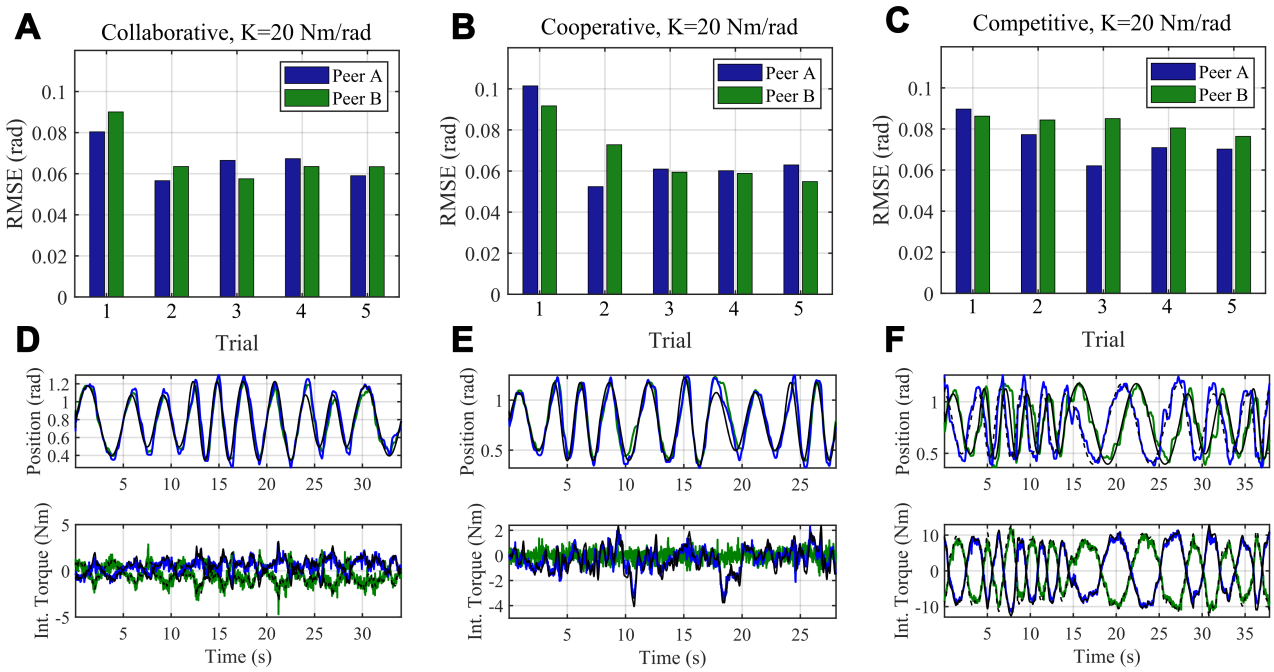


Fig. 7. The $RMSE_\theta$ of the dyadic pair during different interactive behaviors for K = 20 Nm/rad: (A) collaboration, (B) cooperation, and (c) competition tasks. For each interactive condition, there were five trials, each averaged across 10 tracking cycles. (D), (E), and (F) are one representative trials of the position and interaction torque data.

was changed for each behavior because based on pilot data, participants were able to learn (memorize) the trajectory after several trials, namely, the $RMSE_\theta$ saturated after 3 to 4 trials as shown in Fig. 7A-C. Therefore, after 3 to 4 trials, there were no clear learning effects despite additional trials or the change in the interactive behavior. As a result of changing the seed, however, the outcomes for each interactive behavior cannot be compared. Depending on the randomization of the amplitude and frequency, one trajectory can be more challenging than the other. Therefore, the initial $RMSE_\theta$ values for each interactive behaviors and the change in $RMSE_\theta$ across the five trials are different. The order of testing each interactive behavior was also not randomized. This may have allowed participants to get more familiar with the system in one interactive behavior than the other. In future studies, a more challenging desired trajectory will be needed which then can be used across interactive conditions in order to analyze the effects of interactive conditions on individual motor learning and shared task performance. The sequence of testing different interactive conditions will also be randomized.

### *C. Future directions*

In this study, we propose an open-source experimental framework that can be used to systematically test different interactive conditions (i.e., interactive behaviors and level of virtual connections) and investigate the effects on shared task performance and motor learning. To show the feasibility of dyadic studies for different conditions, we have only presented results on shared task performance. In our future studies, we will investigate individual motor learning by comparing the performance (e.g., tracking error, repeatability) of solo trials, in which a participant performs identical tasks without any virtual connections, before and after training with another human via physical interaction.

There are also several studies that report that the skill level of the dyads affected the change in motor performance [1], [3], [7], [12]. It has been reported that improved shared task performance was shown when a participant is paired with a more skilled participant [7], [12]. On the other hand, improved individual motor learning was shown when paired with another novice participant [1], [3], [7], [12]. We plan to investigate the effect of partner characteristics and further study the dyadic interaction between therapists and patients with neurological disorders (e.g., stroke, SCI) in rehabilitation setups. We have also only investigated the effect of virtual springs between human pairs. According to Tanaka et al. [11], the interaction damping also introduced significant differences in task performance. This shows that virtual damping might be an important factor during human-human physical interaction, supporting the need to further investigate this topic.

It has been shown that joint mechanical impedance, which regulates the instantaneous torque response that accompanies changes in joint position, governs the body's response to unexpected disturbances during natural gait [26], [27]. We believe mechanical impedance may also explain human ankle-ankle interaction, where the torque applied by the partner is considered a disturbance. Therefore, in our future studies, we plan to consider the stiffness of the ankle by estimating it from the co-contraction of the agonist and antagonist muscles. This will allow us to investigate how humans strategically sacrifice energy efficiency (i.e., change in metabolic cost from muscle co-contraction) in order to achieve higher task performance.

This will also allow us to investigate the full framework proposed from Jarrasse et al. [17], in which dyads not only consider their own and their partner's task performance but also the metabolic costs. Analyzing the EMG data will also provide information on how active or passive the participants are during the tracking tasks. This can provide information on the engagement level which is key for enhancing neuroplasticity, and to facilitate recovery in patients [28], [29]. With the collective findings on the effect of various interactive conditions, we will develop model-based synthetic controllers to substitute one of the peers and see if similar improvements in motor learning as shown in human-human interaction can be achieved through human-robot interaction.

## V. Conclusion

We presented an open-source experimental framework that can be used to investigate the effect of varying virtual stiffnesses and interactive behaviors between human dyads. We have implemented an interaction torque controller and haptic virtual environment based on an open-source robotic development software stack called CORC [16] to render virtual connections between human dyads. Different interactive behaviors (i.e., collaborative, cooperative, competitive tasks) were emulated by varying the properties of the virtual connection. To validate the infrastructure, we conducted system transparency experiments, virtual spring rendering experiments, and a simple dyadic physical interaction experiment. As future directions, we plan to perform dyadic studies to systematically investigate the effect of interactive conditions, the effects of partner skill levels, and ankle stiffness modulation strategies on shared task performance and individual motor learning.

## References


[1] G. Ganesh, A. Takagi, R. Osu, T. Yoshioka, M. Kawato, and E. Burdet, "Two is better than one: Physical interactions improve motor performance in humans," *Scientific Reports*, vol. 4, pp. 1–7, 2014.

[2] A. Takagi, F. Usai, G. Ganesh, V. Sanguineti, and E. Burdet, "Haptic communication between humans is tuned by the hard or soft mechanics of interaction," *PLoS Computational Biology*, vol. 14, no. 3, pp. 1–17, 2018.

[3] Y. Che, G. M. Haro, and A. M. Okamura, "Two is not always better than one: Effects of teleoperation and haptic coupling," *Proceedings of the IEEE RAS and EMBS International Conference on Biomedical Robotics and Biomechatronics*, vol. 2016-July, pp. 1290–1295, 2016.

[4] J. Wang, A. Chellali, and C. G. Cao, "Haptic Communication in Collaborative Virtual Environments," *Human Factors*, vol. 58, no. 3, pp. 496–508, 2016.

[5] A. Takagi, G. Ganesh, T. Yoshioka, M. Kawato, and E. Burdet, "Physically interacting individuals estimate the partner's goal to enhance their movements," *Nature Human Behaviour*, vol. 1, no. 3, 2017.

[6] N. B. B, A. Keemink, and E. V. Asseldonk, *Haptic Human-Human Interaction Through a Compliant Connection Does Not Improve Motor Learning in a Force Field*. Springer International Publishing, 2018. [Online]. Available: http://dx.doi.org/10.1007/978-3-319-93445-7_29

[7] S. Kager, A. Hussain, A. Cherpin, A. Melendez-Calderon, A. Takagi, S. Endo, E. Burdet, S. Hirche, M. H. Ang, and D. Campolo, "The effect of skill level matching in dyadic interaction on learning of a tracing task," *IEEE International Conference on Rehabilitation Robotics*, vol. 2019-June, pp. 824–829, 2019.

[8] K. Reed, M. Peshkin, M. J. Hartmann, M. Grabowecky, J. Patton, and P. M. Yishton, "Haptically linked dyads are two motor-control systems better than one?" *Psychological Science*, vol. 17, no. 5, pp. 365–366, 2006.

[9] K. B. Reed, M. Peshkin, M. J. Hartmann, J. Patton, P. M. Vishton, and M. Grabowecky, "Haptic cooperation between people, and between people and machines," *IEEE International Conference on Intelligent Robots and Systems*, pp. 2109–2114, 2006.

[10] A. Takagi, C. Bagnato, and E. Burdet, "Facing the partner influences exchanges in force," *Scientific Reports*, vol. 6, pp. 1–6, 2016.

[11] Y. Tanaka and R. Goto, "A robotic rehabilitation system for cooperative motor training: A preliminary study in a balance seesaw task," *2018 IEEE International Conference on Cyborg and Bionic Systems, CBS 2018*, pp. 216–221, 2019.

[12] E. J. Avila Mireles, J. Zenzeri, V. Squeri, P. Morasso, and D. De Santis, "Skill learning and skill transfer mediated by cooperative haptic interaction," *IEEE Transactions on Neural Systems and Rehabilitation Engineering*, vol. 25, no. 7, pp. 832–843, 2017.

[13] A. Sawers and L. H. Ting, "Perspectives on human-human sensorimotor interactions for the design of rehabilitation robots," *Journal of Neuro-Engineering and Rehabilitation*, vol. 11, no. 1, pp. 1–13, 2014.

[14] A. Melendez-Calderon, V. Komisar, and E. Burdet, "Interpersonal strategies for disturbance attenuation during a rhythmic joint motor action," *Physiology Behavior*, vol. 147, pp. 348–358, 2015. [Online]. Available: https://www.sciencedirect.com/science/article/pii/S003193841500253X

[15] R. Groten, D. Feth, R. L. Klatzky, and A. Peer, "The role of haptic feedback for the integration of intentions in shared task execution," *IEEE Transactions on Haptics*, vol. 6, no. 1, pp. 94–105, 2013.

[16] J. Fong, E. B. Küçüktabak, V. Crocher, Y. Tan, K. Lynch, J. Pons, and D. Oetomo, "CANopen Robot Controller (CORC): An open software stack for human robot interaction development," *The International Symposium on Wearable Robotics (WeRob2020)*, vol. 2020, pp. –ss, 2020.

[17] N. Jarrassé, T. Charalambous, and E. Burdet, "A Framework to Describe, Analyze and Generate Interactive Motor Behaviors," *PLoS ONE*, vol. 7, no. 11, 2012.

[18] R. Merletti and P. Di Torino, "Standards for reporting emg data," *J Electromyogr Kinesiol*, vol. 9, no. 1, pp. 3–4, 1999.

[19] S. M. Kidder, F. S. Abuzzahab, G. F. Harris, and J. E. Johnson, "A system for the analysis of foot and ankle kinematics during gait," *IEEE Transactions on Rehabilitation Engineering*, vol. 4, no. 1, pp. 25–32, March 1996.

[20] A. Alamdari and V. Krovi, "Chapter two - a review of computational musculoskeletal analysis of human lower extremities," in *Human Modelling for Bio-Inspired Robotics*, J. Ueda and Y. Kurita, Eds. Academic Press, 2017, pp. 37–73. [Online]. Available: https://www.sciencedirect.com/science/article/pii/B9780128031377000033

[21] Y. Wen, J. Si, X. Gao, S. Huang, and H. Huang, "A New Powered Lower Limb Prosthesis Control Framework Based on Adaptive Dynamic Programming," *IEEE Transactions on Neural Networks and Learning Systems*, vol. 28, no. 9, pp. 2215–2220, sep 2017.

[22] J. Zhang, P. Fiers, K. A. Witte, R. W. Jackson, K. L. Poggensee, C. G. Atkeson, and S. H. Collins, "Human-in-the-loop optimization of exoskeleton assistance during walking," *Science*, vol. 356, no. 6344, pp. 1280–1284, jun 2017.

[23] Y. Ding, M. Kim, S. Kuindersma, and C. J. Walsh, "Human-in-the-loop optimization of hip assistance with a soft exosuit during walking," *Science Robotics*, vol. 3, no. 15, p. eaar5438, feb 2018.

[24] T. Boaventura and J. Buchli, "Acceleration-based transparency control framework for wearable robots," *IEEE International Conference on Intelligent Robots and Systems*, vol. 2016-Novem, pp. 5683–5688, 2016.

[25] Y. Zimmermann, E. B. Kucuktabak, F. Farshidian, R. Riener, and M. Hutter, "Towards Dynamic Transparency : Robust Interaction Force Tracking Using Multi-Sensory Control on an Arm Exoskeleton," *IEEE/RSJ Intenational Conference on Intelligent Robots and Systems (IROS)*, pp. 7417–7424, 2020.

[26] D. A. Winter, "Energy generation and absorption at the ankle and knee during fast, natural, and slow cadences," *Clinical Orthopaedics and Related Research*, vol. No. 175, pp. 147–154, 1983.

[27] A. M. Wind and E. J. Rouse, "Neuromotor Regulation of Ankle Stiffness is Comparable to Regulation of Joint Position and Torque at Moderate Levels," *Scientific Reports*, vol. 10, no. 1, pp. 1–9, 2020.

[28] M. M. Danzl, N. M. Etter, R. O. Andreatta, and P. H. Kitzman, "Facilitating neurorehabilitation through principles of engagement," *Journal of Allied Health*, vol. 41, no. 1, pp. 35–41, 2012.

[29] C. Phillips, "Lifestyle Modulators of Neuroplasticity: How Physical Activity, Mental Engagement, and Diet Promote Cognitive Health during Aging," *Neural Plasticity*, vol. 2017, 2017.